Journal of Materials Education Vol. 39 (5-6): 223-240 (2017)

FORCES ON STRAIGHT DISLOCATIONS – ANALYSIS WITH EXAMPLES

Vlado A. Lubarda

Department of NanoEngineering, University of California, San Diego, La Jolla, CA 92093-0448, USA

ABSTRACT

The derivation of the expression for the configurational or energetic force on a straight dislocation in infinite and finite bodies caused by different sources of stress is revisited from the conceptual and pedagogical points of view, which is of interest for undergraduate and graduate education in materials science and engineering. The classical virtual work approach was first used, followed by the approach based on the potential energy consideration which allows for the incorporation of the effects of image stresses due to the presence of loaded, free, or constrained boundaries. The third utilized approach is based on the evaluation of the J integral. The presented examples include a straight dislocation near a slipping or free boundary of an isotropic half-space or a quarter-space, and a dislocation near a circular or semi-circular hole. The glide and climb components of the dislocation force are evaluated and discussed in each case.

Keywords: *Climb force; dislocation; glide force; image stress; J integral; Peach–Koehler force; potential energy; virtual work; void*

Glossary of symbols:

b	Burgers vector
f	Dislocation force
ξ	Dislocation line vector
ρ	Dislocation core radius
$\mathbf{t}_n$	Traction vector
n, m, e	Unit vectors
$\boldsymbol{\sigma}$	Stress tensor
$\boldsymbol{\sigma}^0$	Applied stress
$\hat{\boldsymbol{\sigma}}$	Image stress tensor
ε	Strain tensor
δW	Virtual work
Π	Potential energy
U	Strain energy
w	Strain energy density
E	Modulus of elasticity
G	Shear modulus
ν	Poisson's ratio
J_β	J integrals
$\delta_{\alpha\beta}$	Kronecker delta

1. INTRODUCTION

Dislocations are crystallographic defects of greatest importance for the analysis of inelastic response of crystalline materials. Their existence was proposed independently by Taylor, Orowan and Polanyi in 1934 in an attempt to explain the shear strength of metals, which was observed to be two or three orders of magnitude lower than the theoretical shear strength.[1-5] The presence of dislocations in crystals was experimentally confirmed by the transmission electron microscopy in the late 1950's and since then dislocations are widely recognized to be the main feature of material structure that controls the plastic yield strength, hardening and ductility of metals.[6-9] Numerous dislocation-based theories were proposed to explain phenomena such as the grain-size dependence of the yield-stress, crack initiation at grain boundaries and inhomogeneities, brittle-to-ductile transition, size effects at micron scale, creep and fatigue behavior, etc.[5-13]

Historically, without any consideration or referral to atomic structure, Vito Volterra in 1907 derived the elastic fields associated with displacement discontinuities in a linearly elastic continuum that correspond to what later became known as the edge and screw dislocations. The stress and strain fields of Volterra dislocations are characterized by an r^{-1} singularity, where r is the distance from the dislocation line, so that the model represents well the elastic fields of a crystalline dislocation sufficiently away from the dislocation line. Very near the dislocation line, nonlinear theories or other remedies are needed to accurately describe the severe distortion of lattice in the dislocation core region. Among them, the most well-known is the Peierls-Nabarro model, which incorporates the size of a spread core or width of a dislocation and the distance between crystallographic planes.[7,9]

The scientific contributions to dislocations by Volterra in 1907 and by Taylor, Orowan and Polanyi in 1934 demonstrate a strong connection between research fields of materials science and mechanics of solids. Another remarkable example of this connection is a celebrated ellipsoidal inclusion problem of Eshelby[14], which keeps engaging researchers from both communities for over sixty years now. An ellipsoidal region (inclusion) undergoes a uniform transformation strain (eigenstrain), such as twinning or martensitic transformation, but due to the constraint from the surrounding material, the inclusion is left in a state of uniform stress. The derived closed form solution for this stress greatly facilitated the developments in the fields of mechanics of heterogeneous materials and mechanics of composites.[15,16] The materials-mechanics linkage in engineering research and education have already been addressed in several publications in the *Journal of Materials Education*.[17-19]

When material is under stress, dislocations move and produce crystallographic slip, which gives rise to plastic deformation. To describe dislocation motion, interaction of dislocations with other dislocations or with other defects, such as foreign atoms, inclusions, grain and phase boundaries, fundamentally important is the so-called energetic or configurational force acting on each portion of the dislocation loop. This force was first derived by Peach and Koehler,[20] and their expression has become known as the Peach-Koehler dislocation force expression. We review in this paper the two-dimensional derivation of the Peach–Koehler force on a straight dislocation, which is simpler and more suitable for the coverage of the topic in undergraduate courses of materials science and mechanical behavior of materials. Some of the derivation may also be appealing for graduate courses. The derivation based on the virtual work is first reviewed[9,20] and then generalized by using the method of the potential energy to include image effects associated with the presence of free or constrained boundaries of the material.[21-25] The third utilized approach is based on the evaluation of the J integral,[26-28] which is suitable for more advanced courses of dislocation theory or

continuum mechanics. The selected examples used to illustrate different approaches include a straight dislocation near free or slipping boundary of a half-space, and a straight dislocation within a quarter- and three-quarter space. These dislocation configurations play important roles in the study of mechanics of thin films and interfaces, grain boundaries, and surface junctions at the corners or re-entrant corners of microstructural elements.[29-32] The non-uniqueness of dislocation force in multiply connected domains is illustrated by an example of a straight dislocation near a cylindrical circular void. This configuration is of importance for the study of void growth by dislocation emission and the material failure by void coalescence and spalling. Numerical determination of dislocation forces near surface steps, circular grooves, or other more complex geometries are discussed. The reference to earlier work on the subject is incorporated throughout the paper.

2. BASIC DISLOCATION CONCEPTS

Figure 1 shows an edge dislocation at the continuum and atomistic levels of description. At the continuum level shown in Fig. 1a, the dislocation is created by cutting a block of material from its left edge to the location of the dislocation line, and by displacing the upper side of the cut by amount b, relative to the lower side of the cut. The imposed displacement discontinuity is known as the Burgers vector of the dislocation. For edge dislocations, the Burgers vector is orthogonal to the dislocation line and is defined by the Burgers circuit shown in Fig. 2. Any cut can be used to create a dislocation by imposing a prescribed displacement discontinuity along it; two cut choices are shown in Fig. 2. On atomistic scale (Fig. 1b), the edge dislocation can be thought as being created by inserting an extra half-plane of atoms midway between two adjacent planes of atoms.[1-5] The dislocation line, orthogonal to the plane of figure, coincides with the bottom row of the extra half-plane of atoms. The heavily distorted region around the dislocation line is the dislocation core.

A screw dislocation is created by displacing the upper side of the cut relative to the lower side of the cut in the direction of the dislocation line. There is no extra half-plane of atoms, but the crystalline lattice is heavily distorted around the dislocation line. The elastic fields of screw dislocation in an infinite medium are particularly simple. The non-vanishing displacement component is $u_3 = b_3\theta/2\pi$, where $\theta \in [0,2\pi]$ is the polar angle in the (r,θ) plane, orthogonal to the dislocation line along the x_3 direction. The corresponding nonvanishing stress is $\sigma_{3\theta} = Gb_3/2\pi r$, demonstrating the previously mentioned r^{-1} singularity along the dislocation line $r = 0$. The shear modulus of the material is denoted by G.

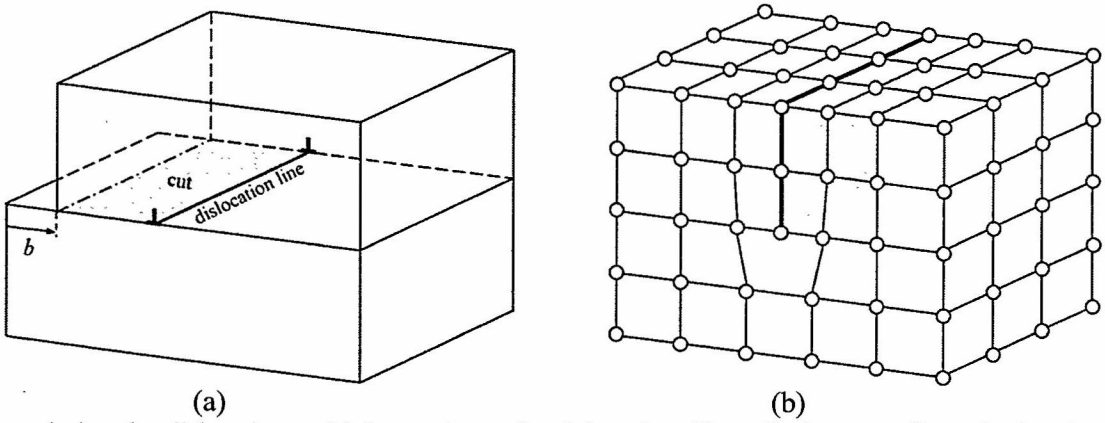

Figure 1. An edge dislocation at: (a) the continuum level, introduced by a displacement discontinuity of amount b along the shown horizontal cut surface, and (b) the atomic level, introduced by insertion of an extra half-plane of atoms.

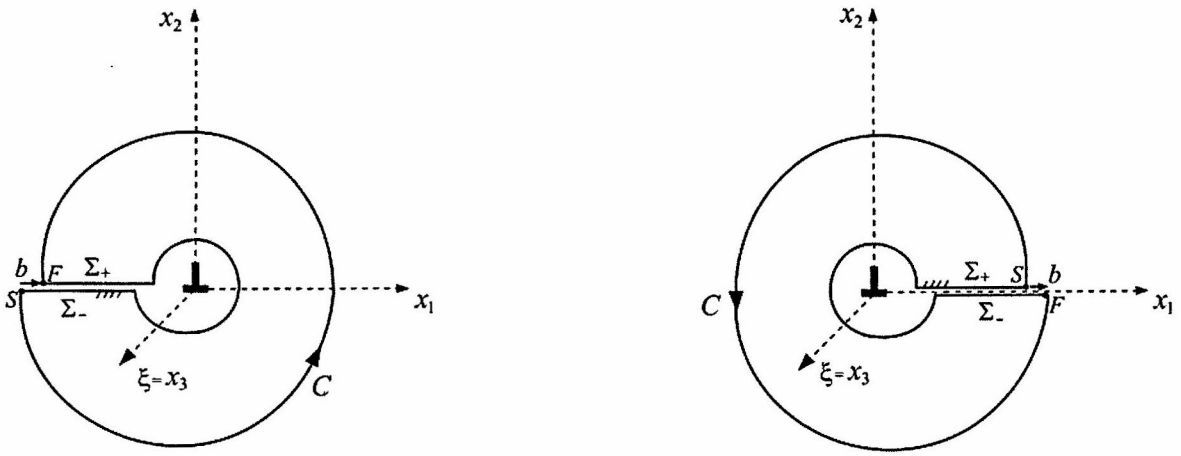

Figure 2. An edge dislocation created by the displacement discontinuity b. In part (a) the upper surface Σ_+ of the cut is displaced by b to the right relative to the lower surface Σ_- along the negative x_1 axis, while in part (b) the displacement discontinuity is imposed along the positive x_1 axis. In each case the chosen direction of the dislocation line vector ξ is out of the plane of figure. The Burgers circuit is right-handed with respect to ξ, it begins at the point S and ends at the point F.

In general, dislocations in crystals are curved, appearing as either closed loops entirely within a crystal, or open loops with their ends exiting at the inner and outer boundaries of the crystal. The dislocation Burgers vector is constant along the dislocation loop, and at an arbitrary point of the loop can be decomposed into its edge component, orthogonal to the loop, and its screw component, tangent to the loop[8-10] (Fig. 4b).

If the length of a Burgers vector is equal to one lattice spacing, the dislocation is referred to as a perfect dislocation (or dislocation of unit strength); otherwise, it is a partial dislocation. It can be shown that the strain energy of dislocation is proportional to the square of the Burgers vector. For example, the strain energy per unit length of a screw dislocation, stored in an annular circular region bounded by the dislocation core radius ρ and a large outer radius R is

$$U = 2\pi\int_{\rho}^{R}\sigma_{3\theta}\varepsilon_{3\theta}r\mathrm{d}r = \frac{\pi}{G}\int_{\rho}^{R}\sigma_{3\theta}^2 r\mathrm{d}r = \frac{Gb_3^2}{4\pi}\ln\frac{R}{\rho}, \tag{1}$$

where $\varepsilon_{3\theta}=\sigma_{3\theta}/2G$ is the shear strain. Thus, in order to minimize the strain energy, the Burgers vector of a dislocation is equal to the shortest lattice translation vector. If is energetically preferred, a perfect dislocation may dissociate into two partial dislocations, separated by a stacking fault, which is referred to as an extended dislocation.[8-10] Under applied stress, dislocations move along the most dense planes of atoms, because the lattice resistance to their motion increases with the spacing between atomic planes.[1-6]

While the motion of a crystalline dislocation within its glide plane is opposed by the lattice friction (Peierls-Nabarro stress),[7,9] the dislocation motion orthogonal to its glide plane is opposed by the barriers to atomic diffusion, because a dislocation can move out of its plane only if the point defects (e.g., vacancies) diffuse to or away from the dislocation, assuming that the temperature of the material is sufficiently high for rapid diffusion.[35] This climb resistance can be estimated by the consideration of the Gibbs energy, which gives the corresponding chemical or osmotic force on a dislocation.

3. PEACH–KOEHLER FORCE ON A STRAIGHT DISLOCATION

Figure 3a shows a straight dislocation of a mixed edge-screw type, located at the point C at large

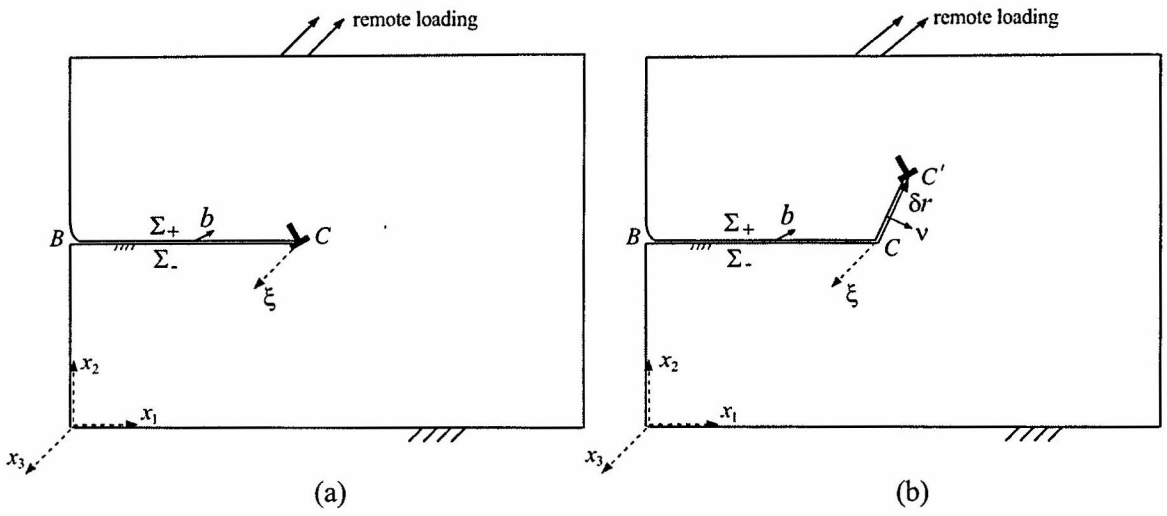

Figure 3. (a) A straight dislocation of a mixed edge-screw type, located at the point C at large distance from the bounding surface of a body. The displacement discontinuity is imposed along the cut from the bounding surface to the point C, by displacing Σ_+ relative to Σ_- by a Burgers vector $\mathbf{b}$. The unit vector of the dislocation line ξ is out of the plane of figure. (b) A nearby position of the dislocation, after it has experienced a displacement $\delta\mathbf{r}$ from C to C'. The unit vector along CC', orthogonal to Σ_+ and directed towards Σ_-, is $\boldsymbol{\nu}$.

distance from the surface of a loaded body, so that the dislocation image stresses[9] due to boundaries can be ignored compared to stresses from the applied load. The Burgers vector of the dislocation consists of the edge and screw components, such that $\mathbf{b} = b_e\mathbf{m} + b_s\boldsymbol{\xi}$, where $b_e = (b_1^2 + b_2^2)^{1/2}$, $\mathbf{m} = \{b_1, b_2, 0\}/b_e$, and $b_s = b_3$. The unit vector along the dislocation line is $\boldsymbol{\xi} = \mathbf{e}_3$. The rectangular coordinates (x_1, x_2, x_3) are used as the background coordinates, with unit vectors $(\mathbf{e}_1, \mathbf{e}_2, \mathbf{e}_3)$. If the stress field in the body (excluding the stress field from the dislocation itself) is denoted by $\boldsymbol{\sigma}$, the work done by it (per unit length of the dislocation), as the dislocation is introduced in the body, is

$$W = \int_B^C \mathbf{t}_{-2} \cdot \mathbf{b}\, dx, \quad \mathbf{t}_{-2} = -\boldsymbol{\sigma} \cdot \mathbf{e}_2 . \tag{2}$$

The cut surface along which the displacement discontinuity is imposed is conveniently selected to be the horizontal surface with a trace BC in the plane of the figure (B being the point at the boundary of the body). In creating the dislocation, the surface Σ_+ is displaced by $\mathbf{b}$ relative to the surface Σ_-. The vector $\mathbf{t}_{-2} = -\mathbf{t}_2$ is the traction vector over the surface element of BC whose normal is in the negative x_2 direction.

Suppose that the dislocation experiences a (virtual) displacement $\delta\mathbf{r}$ from its position C to a nearby position C' (Fig. 3b). The corresponding work is

$$\delta W = \mathbf{t}_\nu \cdot \mathbf{b}\, \delta r = \boldsymbol{\nu} \cdot \boldsymbol{\sigma} \cdot \mathbf{b}\, \delta r, \quad \mathbf{t}_\nu = \boldsymbol{\sigma} \cdot \boldsymbol{\nu} = \boldsymbol{\nu} \cdot \boldsymbol{\sigma}, \tag{3}$$

where $\boldsymbol{\nu}$ is the unit vector orthogonal to $\delta\Sigma_+$ defined by the upper cut along CC', extending the surface cut Σ_+, as indicated in Fig. 1b. The vector $\mathbf{t}_\nu$ is the corresponding traction vector. In view of the geometric vector relation $\boldsymbol{\xi} \times \delta\mathbf{r} = -\boldsymbol{\nu}\delta r$, the substitution into Eq. 3 yields

$$\delta W = -(\boldsymbol{\sigma} \cdot \mathbf{b}) \cdot (\boldsymbol{\xi} \times \delta\mathbf{r}) = -\delta\mathbf{r} \cdot [(\boldsymbol{\sigma} \cdot \mathbf{b}) \times \boldsymbol{\xi}] . \tag{4}$$

Consequently, by defining the force on a straight dislocation $\mathbf{f}$ such that $\mathbf{f} \cdot \delta\mathbf{r} = -\delta W$, the comparison with Eq. 4 establishes the celebrated Peach–Koehler[20] expression

$$\mathbf{f} = (\boldsymbol{\sigma} \cdot \mathbf{b}) \times \boldsymbol{\xi} . \tag{5}$$

The same structure of the expression holds for dislocation loops, provided that $\boldsymbol{\xi}$ is tangential

to the loop (Fig. 4). The Peach–Koehler expression plays a fundamental role in materials science studies of dislocation motion and interaction of dislocations with other dislocations or other material defects, such as inhomogeneities, voids, and grain boundaries.[6-10]

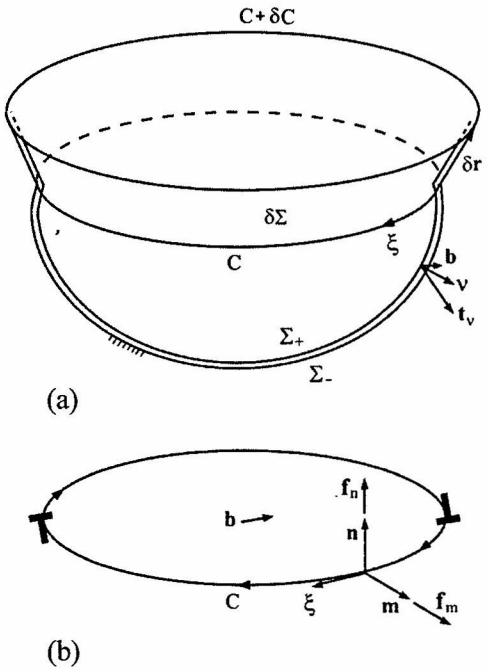

Figure 4. (a) The dislocation loop C created by a cut surface below the plane of the loop. The surface Σ_+ is displaced by a Burgers vector **b** relative to the surface Σ_-. The dislocation line vector along the loop is $\boldsymbol{\xi}$. The traction vector over Σ_+ is $\mathbf{t}_\nu$, where $\boldsymbol{\nu}$ is the unit vector orthogonal to Σ_+ and directed towards Σ_-. A nearby configuration of the dislocation loop is C+δC, obtained from C by a displacement variation $\delta\mathbf{r}$ specified along the loop. The surface connecting C and C+δC is $\delta\Sigma$. (b) The glide and climb components of the dislocation force along a planar dislocation loop C in the plane whose unit normal is **n**. The unit vector **m** is in the plane of the loop, orthogonal to it and directed outward from it. The projections of the dislocation force **f** onto **m** and **n** are its glide and climb components, $\mathbf{f}_{glide} = \mathbf{f}_m$ and $\mathbf{f}_{climb} = \mathbf{f}_n$.

If the image stresses from the boundary of the body ($\hat{\boldsymbol{\sigma}}$) and the stresses due to interaction of the dislocation with other dislocations or other defects in the body ($\boldsymbol{\sigma}^{int}$) are included in the analysis, the Peach-Koehler expression for the dislocation force takes the form[18-21]

$$\mathbf{f} = [(\boldsymbol{\sigma}^0 + \hat{\boldsymbol{\sigma}} + \boldsymbol{\sigma}^{int}) \cdot \mathbf{b}] \times \boldsymbol{\xi}\,, \tag{6}$$

where $\boldsymbol{\sigma}^0$ represents the stress contribution from the external load only.

In some studies, and textbooks on dislocations,[9,33] one direction of the dislocation line vector is taken as positive, while in others,[34,35] the opposite direction is taken as positive. Although both directions are permissible choices, a care is needed to properly identify the corresponding direction of the Burgers vector of the dislocation.[36]

3.1 Glide and climb components of dislocation force

Since for a straight dislocation $\boldsymbol{\xi} = \mathbf{e}_3$, the rectangular (x_1, x_2, x_3) components of the corresponding dislocation force are, from Eq. 5,

$$\begin{aligned} f_1 &= \sigma_{21} b_1 + \sigma_{22} b_2 + \sigma_{23} b_3\,, \\ f_2 &= -(\sigma_{11} b_1 + \sigma_{12} b_2 + \sigma_{13} b_3)\,, \\ f_3 &= 0\,. \end{aligned} \tag{7}$$

The force **f** can also be decomposed into its glide component $\mathbf{f}_{glide} = (\mathbf{f}\cdot\mathbf{m})\mathbf{m}$ and its climb component $\mathbf{f}_{climb} = (\mathbf{f}\cdot\mathbf{n})\mathbf{n}$ (Fig. 4b), such that $\mathbf{f} = \mathbf{f}_{glide} + \mathbf{f}_{climb}$, where

$$\begin{aligned} \mathbf{n} &= \frac{1}{b_e}(\boldsymbol{\xi}\times\mathbf{b}) = \frac{1}{b_e}\{-b_2, b_1, 0\}\,, \\ \mathbf{m} &= \mathbf{n}\times\boldsymbol{\xi} = \frac{1}{b_e}\{b_1, b_2, 0\}\,. \end{aligned} \tag{8}$$

Equation 9 (next page) readily follows.

$$f_{glide} = \frac{1}{b_e}\left[(\sigma_{22}-\sigma_{11})b_1b_2 + \sigma_{12}(b_1^2 - b_2^2) + \sigma_{32}b_3b_1 - \sigma_{31}b_3b_2\right],$$
$$f_{climb} = -\frac{1}{b_e}\left[\sigma_{11}b_1^2 + \sigma_{22}b_2^2 + 2\sigma_{12}b_1b_2 + \sigma_{31}b_3b_1 + \sigma_{32}b_3b_2\right]. \quad (9)$$

If φ is the angle between the edge component of the dislocation and the x_1 axis, then $b_1 = b_e\cos\varphi$, $b_2 = b_e\sin\varphi$, and Eq. 9 can be recast as

$$f_{glide} = \sigma_{mn}b_e + \sigma_{3n}b_3, \quad f_{climb} = -(\sigma_{mm}b_e + \sigma_{3m}b_3), \quad (10)$$

where

$$\sigma_{mn} = \frac{1}{2}(\sigma_{22}-\sigma_{11})\sin 2\varphi + \sigma_{12}\cos 2\varphi, \quad \sigma_{mm} = \sigma_{11}\cos^2\varphi + \sigma_{22}\sin^2\varphi + \sigma_{12}\sin 2\varphi,$$
$$\sigma_{3m} = \sigma_{32}\sin\varphi + \sigma_{31}\cos\varphi, \quad \sigma_{3n} = \sigma_{32}\cos\varphi - \sigma_{31}\sin\varphi. \quad (11)$$

Alternatively, Eq. 10 can be derived directly from Eq. 5 by expressing the stress tensor $\boldsymbol{\sigma}$ and the Burgers vector $\mathbf{b}$ in the coordinate system specified by unit vectors $(\mathbf{m},\mathbf{n},\mathbf{e}_3)$. Further discussion with specific evaluations of glide and climb forces will be given in section 4.

3.2 Image force on dislocation near a slipping boundary

Figure 5a shows a straight dislocation with a Burgers vector $\{b_1,b_2,b_3\}$ at a distance h from a slipping boundary of a half-space. The slipping boundary prevents the normal displacement $(u_1 = 0, \sigma_{11} \neq 0)$, but allows tangential displacements $(u_2 \neq 0, u_3 \neq 0, \sigma_{12} = \sigma_{13} = 0)$. The dislocation is created by the displacement discontinuity along the x_1 axis from $x_1 = h$ to infinity.

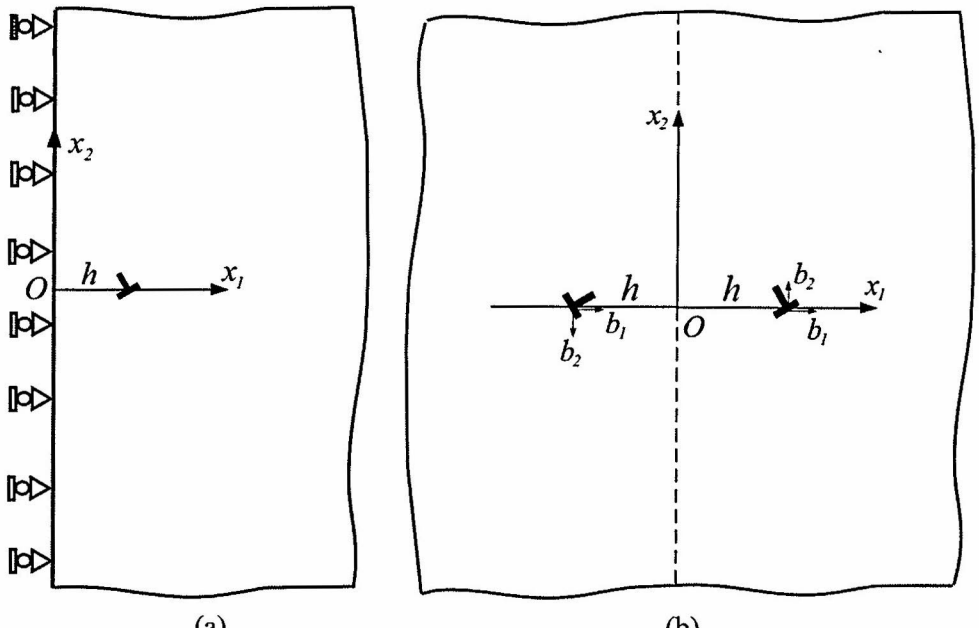

Figure 5. (a) A straight dislocation with a Burgers vector $\{b_1,b_2,b_3\}$ at a distance h from the sliding boundary of an isotropic half-space, which can be a model for a grain boundary incapable of supporting the shear stress. (b) The solution to the problem in Fig. 2a is obtained by superimposing the infinite-medium elastic fields of the actual dislocation with a Burgers vector $\{b_1,b_2,b_3\}$ and an image dislocation with a Burgers vector $\{b_1,-b_2,-b_3\}$, placed at point $(x_1 = -h, x_2 = 0)$.

The complete elastic solution for this problem can be obtained by placing in an infinite medium an image dislocation with a Burgers vector $\{b_1, -b_2, -b_3\}$ at point ($x_1 = -h$, $x_2 = 0$, Fig. 5b), because two dislocations together produce neither shear stress nor horizontal displacement along the plane $x_1 = 0$ in an infinite medium ($\sigma_{12} = \sigma_{13} = 0$, $u_1 = 0$).

In the absence of other stresses, the Peach–Koehler dislocation force is due to image stresses ($\hat{\sigma}_{ij}$) only, caused by the interaction of dislocation with the boundary, i.e.,

$$f_1 = \hat{\sigma}_{21} b_1 + \hat{\sigma}_{22} b_2 + \hat{\sigma}_{23} b_3 . \tag{12}$$

The stress components $\hat{\sigma}_{ij}$ at the dislocation position $x_1 = h$ are equal to those produced in an infinite medium by the image dislocation $\{b_1, -b_2, -b_3\}$ at $x_1 = -h$. These are[9]

$$\hat{\sigma}_{21} = \frac{Gb_1}{2\pi(1-\nu)} \frac{1}{2h},$$

$$\hat{\sigma}_{22} = -\frac{Gb_2}{2\pi(1-\nu)} \frac{1}{2h}, \tag{13}$$

$$\hat{\sigma}_{23} = -\frac{Gb_3}{2\pi} \frac{1}{2h},$$

where G is the shear modulus and ν is the Poisson ratio. The substitution of Eq. 13 into Eq. 12 yields

$$f_1 = \frac{G}{4\pi h}\left(\frac{b_1^2 - b_2^2}{1-\nu} - b_3^2\right). \tag{14}$$

The dislocation is in equilibrium if $b_1^2 = b_2^2 + (1-\nu) b_3^2$. For example, a pure edge dislocation is in equilibrium if its Burgers vector is oriented so that $b_1 = \pm b_2$.

Alternatively, Eq. 14 can be deduced from the analysis of an edge dislocation near a circular inclusion with a slipping interface,[37] by letting the radius of a rigid inclusion to be much greater than the distance of the dislocation from the interface. For slipping interface, the contribution from the screw dislocation component to the dislocation force is the same as in the case of a traction-free boundary.[38]

4. DISLOCATION FORCE BY POTENTIAL ENERGY CONSIDERATION

Consider an infinitely thick rectangular block of isotropic elastic material having a width a and height h. An edge dislocation of a Burgers vector b_1 resides at distance x_1 from the left side of the block (Fig. 6a). The dislocation is introduced by the slip discontinuity b_1 along the horizontal cut from $x_1 = 0$ to the current position x_1; the upper side of the cut is displaced by b_1 to the right relative to the lower side of the cut. The entire block is subjected to external uniform shear stress of magnitude σ_{12}^0. The potential energy of a dislocated block is

$$\Pi = \Pi^0 + \widetilde{U}_c + \widetilde{U}_{\infty-c} - \frac{1}{2} b_1 \int_0^{x_1} \hat{\sigma}_{12} \mathrm{d}x_1 - b_1 \sigma_{12}^0 x_1 , \tag{15}$$

where $\hat{\sigma}_{12}$ stands for the image shear stress due to the boundaries of the block. The strain energy around the dislocation in an infinite medium, stored within the dislocation core of small radius ρ, is denoted by $\widetilde{U}_c$. The infinite-medium strain energy outside of the dislocation core, stored within a circular cylinder of large radius R, is[9,10]

$$\widetilde{U}_{\infty-c} = \frac{Gb_1^2}{4\pi(1-\nu)} \ln \frac{R}{\rho} . \tag{16}$$

Finally, Π^0 in Eq. 15 is the potential energy of the block without a dislocation, i.e.,

$$\Pi^0 = \frac{1}{2}\sigma_{12}^0 \gamma_{12}^0 (ah) - \sigma_{12}^0 (h\gamma_{12}^0) a , \quad \gamma_{12}^0 = \frac{\sigma_{12}^0}{G} , \tag{17}$$

where $\gamma_{12}^0 = 2\varepsilon_{12}^0$ is the engineering shear strain in the block. The horizontal displacement of the upper side of the block relative to the lower side is $u_1^0 = h\gamma_{12}^0$.

The change of the potential energy due to an additional slip of the dislocation (δx_1) is

$$\delta\Pi = -b_1(\hat{\sigma}_{12} + \sigma_{12}^0)\delta x_1 . \tag{18}$$

Since the dislocation force f_1 is defined by $f_1 \delta x_1 = -\delta\Pi$, the comparison with Eq. 18

establishes the expression

$$f_1 = (\hat{\sigma}_{12} + \sigma_{12}^0) b_1 \,. \qquad (19)$$

Being parallel to the Burgers vector, this is a glide force on the dislocation.

If the dislocation is deep inside a large block, so that the image stress $\hat{\sigma}_{12} << \sigma_{12}^0$, only then we have the (approximate) expression for the dislocation force $f_1 = \sigma_{12}^0 b_1$, commonly listed in the undergraduate textbooks of materials science and mechanical behavior of materials.[1-5] Near the free surface of the block, however, the image stress $\hat{\sigma}_{12}$ can easily be comparable or exceed the applied stress σ_{12}^0, and in such cases the proper expression for the dislocation force is given by Eq. 19.

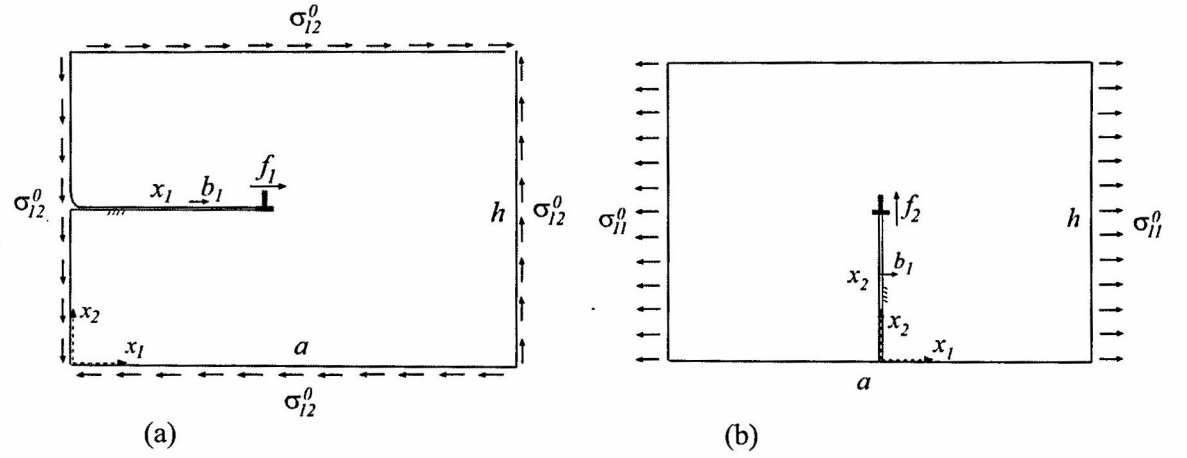

Figure 6. (a) An infinitely thick rectangular block of width a and height h. The block is under applied uniform shear stress σ_{12}^0. An edge dislocation with a Burgers vector b_1 resides at the distance x_1 from the left side. The dislocation is introduced by the slip discontinuity b_1 along the horizontal cut from $x_1 = 0$ to the current x. Shown is the glide component of the force acting on the dislocation ($f_1 > 0$). (b) The same block as in (a), under applied uniform normal stress σ_{11}^0. The edge dislocation with a Burgers vector b_1, located at the distance x_2 from the lower side of the block, is created by the displacement discontinuity b_1 along the vertical cut below the dislocation. Shown is the climb component of the force acting on the dislocation ($f_2 < 0$).

It is appealing to evaluate the average dislocation force required to drive the dislocation through the entire block, from $x = 0$ to $x = a$. This can be accomplished by first noting that

$$\int_0^a f_1 \mathrm{d}x_1 = -(\Pi_{x_1=a} - \Pi_{x_1=0}) = \frac{1}{2} b_1 \int_0^a \hat{\sigma}_{12} \mathrm{d}x_1 + b_1 \sigma_{12}^0 a \,, \qquad (20)$$

from which the average force is

$$\bar{f}_1 = \frac{1}{a}\int_0^a f_1 \mathrm{d}x_1 = \frac{1}{a}\left(\frac{1}{2} b_1 \int_0^a \hat{\sigma}_{12} \mathrm{d}x_1 + b_1 \sigma_{12}^0 a\right). \qquad (21)$$

On physical grounds, the image stress $\hat{\sigma}_{12}$ must be an odd function of the horizontal coordinate measured from the middle of the block ($x_1 = a/2$), so that $\int_0^a \hat{\sigma}_{12} \mathrm{d}x_1 = 0$, and the change of potential energy is simply the negative of (plastic) work done by applied stress σ_{12}^0 on plastic shear strain (b_1/h), i.e., $\Pi_{x_1=a} - \Pi_{x_1=0} = -\sigma_{12}^0 (b_1/h) a h = -\sigma_{12}^0 b_1 a$. Consequently, the average force acting on the dislocation, as it glides from the left to the right side of the block, is exactly $\bar{f}_1 = \sigma_{12}^0 b_1$.

4 CLIMB FORCE

Figure 6b shows a rectangular block of width a and height h, under applied uniform normal stress σ_{11}^0, with an edge dislocation of the Burgers vector b_1 at a distance x_2 from the lower side of the block. The dislocation is introduced by the displacement discontinuity b_1 along the vertical cut below the dislocation; the left side of the cut is displaced by b_1 to the right relative to the right side of the cut, and the overlapping material imagined to be scraped out. The total potential energy is

$$\Pi = \Pi^0 + \widetilde{U}_c + \widetilde{U}_{\infty-c} + \frac{1}{2}b_1\int_0^{x_2}\hat{\sigma}_{11}\mathrm{d}x_2 + b_1\sigma_{11}^0 x_2 \quad (22)$$

where

$$\Pi^0 = \frac{1}{2}\sigma_{11}^0\varepsilon_{11}^0(ah) - \sigma_{11}^0(a\varepsilon_{11}^0)h, \qquad \varepsilon_{11}^0 = (1-\nu^2)\frac{\sigma_{11}^0}{E}. \quad (23)$$

The modulus of elasticity is E, while the horizontal displacement of the right side of the block relative to its left side is $u_1^0 = a\varepsilon_{11}^0$.

The change of potential energy, associated with an additional displacement of the dislocation (δx_2) is

$$\delta\Pi = b_1(\hat{\sigma}_{11} + \sigma_{11}^0)\delta x_2. \quad (24)$$

Since the dislocation force is defined by $f_2\delta x_2 = -\delta\Pi$, it follows that

$$f_2 = -(\hat{\sigma}_{11} + \sigma_{11}^0)b_1. \quad (25)$$

Being orthogonal to the Burgers vector, this is a climb force on the dislocation. It is directed downwards ($f_2 < 0$) for $b_1 > 0$ and $\hat{\sigma}_{11} + \sigma_{11}^0 > 0$, and vice versa.

If the dislocation is deep inside a large block of material so that the image stress is negligible ($\hat{\sigma}_{11} << \sigma_{11}^0$), the expression for the climb force is given approximately by $f_2 = -\sigma_{11}^0 b_1$, which is directed downwards for $b_1 > 0$ and $\sigma_{11}^0 > 0$. In the context of a crystalline dislocation, this means that the climb force acts in the direction opposite to the direction of the inserted extra half-plane of atoms, provided that $\sigma_{11}^0 > 0$. It is noted that the Weertman and Weertman[35] expression 3.13 on page 58 for the climb force is $f_2 = \sigma_{11}^0 b_1$, but their b_1 is opposite in direction to ours, although both describe the same dislocation.

Physically, the climb in a real crystal occurs by diffusion (emission or absorption) of lattice vacancies, but a discussion of these processes is beyond the scope of the present paper.[9,35] One may, however, intuitively argue that the increased tensile state of stress below the positive edge dislocation, caused by the applied stress $\sigma_{11}^0 > 0$, facilitates the absorption of extra atoms below the dislocation, on the expense of the correspondingly increased vacancy concentration surrounding the dislocation, which contributes to the downward direction of the climb force in Fig. 6b ($f_2 < 0$).

To evaluate the average dislocation force required to drive dislocation throughout the block, from $x_2 = 0$ to $x_2 = h$ (which results in the plastic strain $-b_1/a$, associated with the removed sheet of material of thickness b_1), we first note that

$$\int_0^h f_2\mathrm{d}x_2 = -(\Pi_{x_2=h} - \Pi_{x_2=0}) = -\left(\frac{1}{2}b_1\int_0^h\hat{\sigma}_{11}\mathrm{d}x_2 + b_1\sigma_{11}^0 h\right), \quad (26)$$

from which we derive

$$\bar{f}_2 = \frac{1}{h}\int_0^h f_2\mathrm{d}x_2 = -\frac{1}{h}\left(\frac{1}{2}b_1\int_0^h\hat{\sigma}_{11}\mathrm{d}x_2 + b_1\sigma_{11}^0 h\right). \quad (27)$$

The image stress $\hat{\sigma}_{11}$ must be an odd function of the vertical coordinate measured from the middle of the block ($x_2 = h/2$), so that $\int_0^h\hat{\sigma}_{11}\mathrm{d}x_2 = 0$, and the change in potential energy is simply the negative of (plastic) work done by applied stress σ_{11}^0 on plastic longitudinal strain $(-b_1/a)$, i.e.,

$$\Pi_{x_2=h} - \Pi_{x_2=0} = \sigma_{11}^0 (b_1/a)ah = \sigma_{11}^0 b_1 h \quad .$$

Consequently, the average force acting on the dislocation, as it moves from lower to upper side of the block, is exactly $\bar{f}_2 = -\sigma_{11}^0 b_1$.

5. DISLOCATION FORCE BY J INTEGRAL EVALUATION

The J_β integrals represent the energetic or configurational forces associated with infinitesimal translations of a material defect in x_β directions.[26-28] They are defined by

$$J_\beta = \oint (w\delta_{\alpha\beta} - \sigma_{\alpha\gamma} u_{\gamma,\beta} - \sigma_{\alpha 3} u_{3,\beta}) n_\alpha \, dl, \quad (\alpha,\beta) = 1,2 , \tag{28}$$

where the integration is taken over a closed contour surrounding a defect, whose infinitesimal element is dl with the outward normal n_α. The displacement components are denoted by u_α, the comma specifies the indicated partial derivative, and $\delta_{\alpha\beta}$ are the components of the Kronecker delta tensor. The summation convention is implied over a repeated index. The strain energy density is

$$w = \frac{1}{2}\sigma_{\alpha\beta}\varepsilon_{\alpha\beta} + \sigma_{3\gamma}\varepsilon_{3\gamma}. \tag{29}$$

The strain components are related to stress components by Hooke's law

$\varepsilon_{\alpha\beta} = (\sigma_{\alpha\beta} - \nu\sigma_{\gamma\gamma}\delta_{\alpha\beta})/2G$ and

$\varepsilon_{3\gamma} = \sigma_{3\gamma}/2G$, with $\sigma_{\gamma\gamma} = \sigma_{11} + \sigma_{22}$.

If a defect is a straight dislocation, the J_β integrals represent the components of the dislocation force in the x_β directions. The J_β integrals were effectively used to address many problems, particularly in fracture mechanics, including dislocation-crack interactions.[39,40]

5.1 Image force on a straight dislocation near a free surface

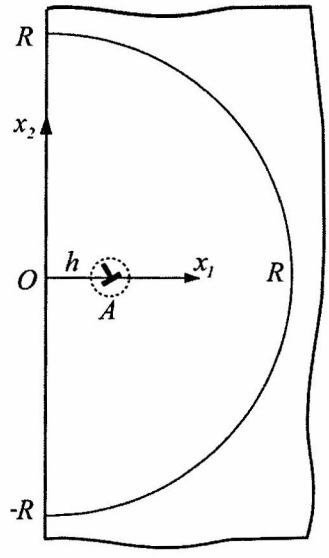

Figure 7. A straight dislocation at point A, a distance h from a free boundary of an isotropic half-space. The J_1 integral can be conveniently evaluated along a closed contour which consists of a long boundary segment from $x_1 = -R$ to $x_1 = R$, completed by a large semicircle of radius $R >> h$. The contribution to J_1 from a large semicircle of radius R vanishes, because the distance h is not observed from such large distances and a dislocation acts as if it has exited the material.

Figure 7 shows a straight dislocation with a Burgers vector $\{b_1, b_2, b_3\}$ at a distance h from the free boundary of a half-space $(\sigma_{11} = \sigma_{12} = \sigma_{13} = 0)$. The dislocation is created by the displacement discontinuity along the x_1 axis from $x_1 = h$ to infinity. By taking a closed contour to consist of the segment $(-R, R)$ along the free boundary and a semicircle of radius R, centered at O, rather than a small (dashed) circle around A, it follows that in the limit as $R \to \infty$ the non-vanishing contribution to J_1 integral comes only from stresses along the boundary $x_1 = 0$, such that Eq. 28 gives

$$J_1 = -\frac{1}{2G}\left[(1-\nu)\int_0^\infty \sigma_{22}^2(0, x_2)\mathrm{d}x_2 + 2\int_0^\infty \sigma_{32}^2(0, x_2)\mathrm{d}x_2\right]. \tag{30}$$

The integral $J_2 = 0$ because there is no change of energy associated with the change of dislocation position along the x_2 direction.

The stress components $\sigma_{22}(0,x_2)$ and $\sigma_{32}(0,x_2)$ along the free surface $x_1=0$ can be determined by either using the complete solution for the stress field,[42] or the procedure which enables the calculation of $\sigma_{22}(0,x_2)$ and $\sigma_{32}(0,x_2)$ solely in terms of the infinite-medium stresses, without solving the entire boundary-value problem.[43,44] In either case one obtains

$$\sigma_{22}(0,x_2)=\frac{4Ghx_2}{\pi(1-\nu)}\frac{b_1h-b_2x_2}{(h^2+x_2^2)^2},$$
$$\sigma_{32}(0,x_2)=-\frac{Gb_3}{\pi}\frac{h}{h^2+x_2^2}. \tag{31}$$

The substitution of Eq. 31 into Eq. 30 and integration then gives

$$f_1=-\frac{G}{4\pi h}\left(\frac{b_1^2+b_2^2}{1-\nu}+b_3^2\right), \tag{32}$$

in agreement with the classical result of Head,[42] obtained from the Peach–Koehler expressions and the entire solution of the considered boundary-value problem.

An alternative, even simpler derivation of the force exerted on a dislocation by the free surface of a half-space can be obtained from the consideration of the so-called M conservation integral, as in the Rice's[41] analysis of dislocation force near a bi-material interface, or from the corresponding Barnett and Lothe[45] formula expressed in terms of the pre-logarithmic energy factors. Details of these calculations can be found in a recent paper,[46] but this coverage is beyond the background of undergraduate engineering students and is recommended only for graduate courses of solid mechanics and materials. Related aspects of the stress and energy analysis of dislocation arrays near the free surfaces and bi-material interfaces are also worthwhile consulting.[47]

5.2 Further comments on glide and climb forces

Figure 8a shows a straight dislocation with a Burgers vector $\{b_1,0,b_3\}$ at a distance h from the free surface ($x_1=0$) of a half-space $x_1\geq 0$. Figure 8b shows the same dislocation at a distance h (along the x_1 axis) from the free surface ($x_2=x_1\cot\varphi$) of a half-space $x_2-x_1\cot\varphi<0$. We prove below that the glide force on the dislocation is the same in both cases and given by

$$f_1=-\frac{G}{4\pi h}\left(\frac{b_1^2}{1-\nu}+b_3^2\right), \tag{33}$$

independently of the angle $-\pi/2<\varphi<\pi/2$. The proof of this result is a corollary of Eq. 31. Indeed, the total force acting on the dislocation in Fig. 8b is directed along the n-direction (orthogonal to the free boundary) and is given by

$$f_n=-\frac{G}{4\pi a}\left(\frac{b_1^2}{1-\nu}+b_3^2\right), \quad a=h\cos\varphi, \tag{34}$$

where a is the normal distance of the dislocation from the free boundary. The glide component of this force is $f_1=f_n\cos\varphi$, thus Eq. 33.

The climb component of the dislocation force in Fig. 8b is $f_2=-f_n\sin\varphi$, which gives

$$f_2=\frac{G}{4\pi h}\left(\frac{b_1^2}{1-\nu}+b_3^2\right)\tan\varphi. \tag{35}$$

For $0<\varphi<\pi/2$ the climb force is directed upwards, and for $-\pi/2<\varphi<0$ downwards.

For completeness of this analysis, it is pointed out that the radial force on a straight dislocation in a quarter- or three-quarter space shown in Fig. 9, directed along the radius r from the apex O, is given by

$$f_r=\frac{G}{4\pi r}\left(\frac{b_1^2+b_2^2}{1-\nu}+b_3^2\right). \tag{36}$$

This result follows from the M integral consideration, analogous to the analysis of a dislocation in a bi-material wedge.[41] It can be furthermore shown that the radial component of dislocation force toward the tip of a wedge of any angle, including a semi-infinite crack,[48] is also given by Eq. 36.

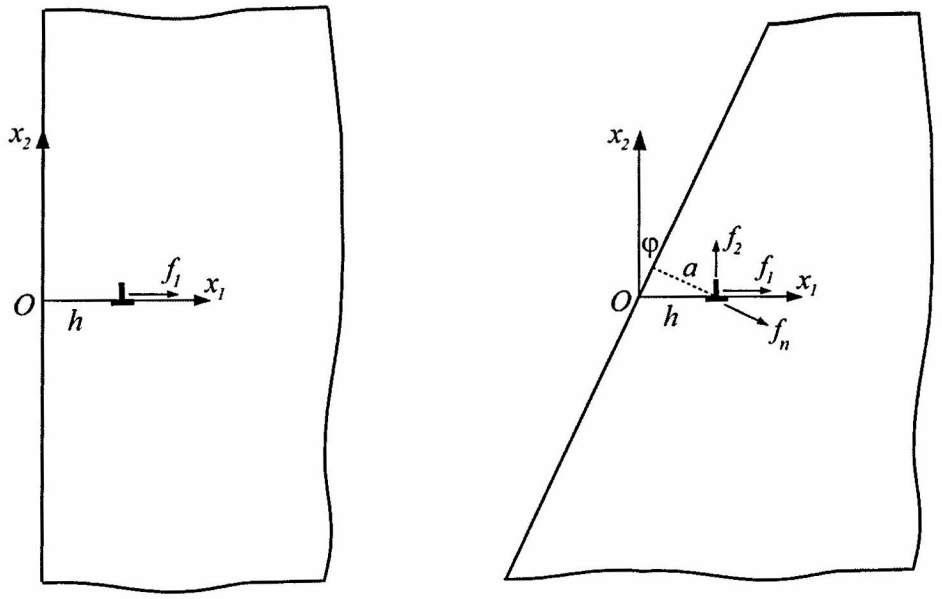

(a) (b)

Figure 8. (a) A straight dislocation with a Burgers vector $\{b_1, 0, b_3\}$ at a distance h from the free surface of a half-space. (b) The same dislocation at a distance h (along the x_1 axis) from the inclined free surface of a half-space at an angle φ from the x_2 axis. The glide and climb components of the dislocation force are f_1 and f_2. The total dislocation force is f_n, orthogonal to the free surface.

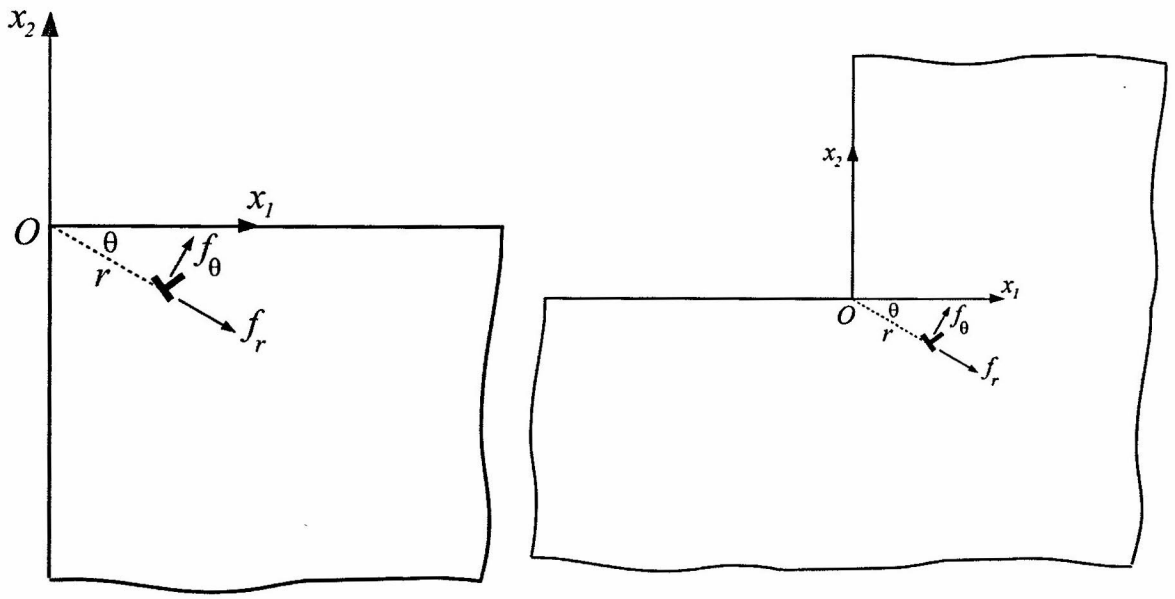

(a) (b)

Figure 9 A straight dislocation in (a) quarter-space, and (b) three-quarter space. The former is a model for a junction of two free surfaces, and the latter for a re-entrant corner of a microstructural element. The radial and circumferential components of the dislocation force are denoted by f_r and f_θ.

The circumferential component f_θ has to be determined numerically for a given angle θ (except for $\theta = 45^\circ$ and $b_1 = \pm b_2$, when $f_\theta = 0$). For a pure screw dislocation ($b_1 = b_2 = 0$) in a quarter-space there is an analytical solution based on the method of image dislocations.[49]

6. DISLOCATION NEAR A CIRCULAR VOID

Elastic stress and strain fields for a dislocation in multiply connected regions depend on a cut used to create a dislocation. If the connectivity of a region is n, there are that many different fields.[50,51] This is illustrated for a dislocation near a circular cylindrical void in an infinite medium in Fig. 10. If a straight dislocation is created by a cut from A to infinity (Fig. 10a), the components of the dislocation force are[49]

$$\begin{aligned} f_1 &= -\frac{G}{2\pi(1-\nu)}\,\frac{a^2}{d(d^2-a^2)}\left[(2-\frac{a^2}{d^2})b_1^2 + b_2^2 + (1-\nu)b_3^2\right], \\ f_2 &= \frac{Gb_1b_2}{2\pi(1-\nu)}\,\frac{a^2}{d^3}\,. \end{aligned} \tag{37}$$

The radius of the void is denoted by a and d is the distance of the dislocation from the center of the void. If the dislocation is created by a cut from the surface of the void to the center of dislocation at A (Fig. 10b), the components of the dislocation force are[42]

$$\begin{aligned} f_1 &= -\frac{G}{2\pi(1-\nu)}\,\frac{d}{d^2-a^2}\left[b_1^2 + (1+\frac{a^2}{d^2}-\frac{a^4}{d^4})b_2^2 + (1-\nu)b_3^2\right], \\ f_2 &= \frac{Gb_1b_2}{2\pi(1-\nu)}\,\frac{1}{d}\,(2-\frac{a^2}{d^2})\,. \end{aligned} \tag{38}$$

Expressions 38 played an important role in the analysis of void growth by dislocation emission from its surface and consequent material failure by void coalescence and spalling.[53,54]

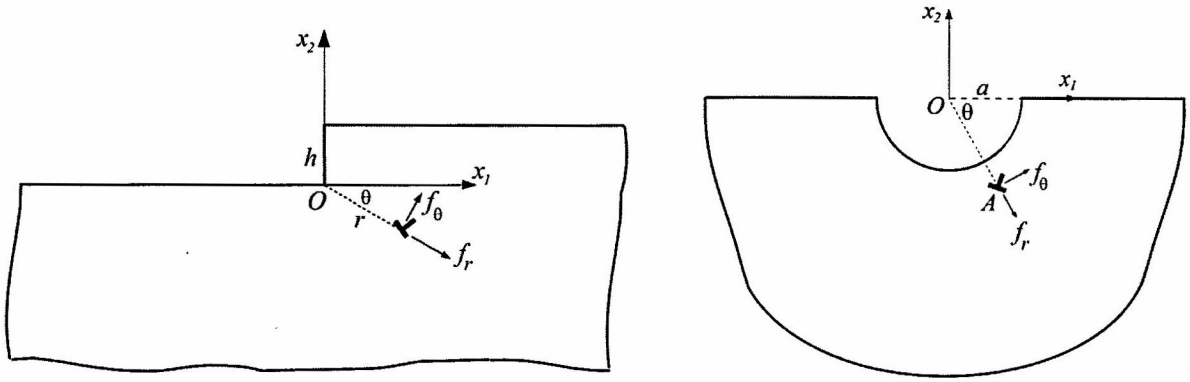

(a) (b)

Figure 10. A straight dislocation near a surface step of a half-space (a), or near a half-space weakened by a semi-circular groove (b). The radial and circumferential components of the dislocation force are denoted by f_r and f_θ.

The ratios of the forces f_1, calculated from Eq. 37 and 38, for each of the components of the Burgers vector, are

$$\left(\frac{f_1^{\mathrm{D}}}{f_1^{\mathrm{L}}}\right)_{b_1} = \frac{a^2}{d^2}\left(2-\frac{a^2}{d^2}\right),$$

$$\left(\frac{f_1^{\mathrm{D}}}{f_1^{\mathrm{L}}}\right)_{b_2} = \frac{a^2}{d^2}\left(1+\frac{a^2}{d^2}-\frac{a^4}{d^4}\right)^{-1}, \qquad (39)$$

$$\left(\frac{f_1^{\mathrm{D}}}{f_1^{\mathrm{L}}}\right)_{b_3} = \frac{a^2}{d^2}.$$

Since $a<d$, it follows that $f_1^{\mathrm{D}} < f_1^{\mathrm{L}}$ for all three types of dislocations. The glide and climb components of the dislocation force are easily determined from $f_{gl} = f_1\cos\varphi + f_2\sin\varphi$ and $f_{cl} = -f_1\sin\varphi + f_2\cos\varphi$, where $\tan\varphi = b_2/b_1$

The derivation of expressions 37 and 38 is based on the use of the Airy stress function[55] and is quite lengthy, but their special cases corresponding to a pure screw dislocation are simple and can be covered even in an undergraduate materials course. In this case, the solution is readily obtained by the method of image dislocations. For the cut shown in Fig. 10a, two image dislocations are needed: a positive screw dislocation at O and a negative screw dislocation at the conjugate point, which is at distance a^2/d from the center of the void along the x_1 direction. For the cut shown in Fig. 10b, only one image dislocation is needed, a negative screw dislocation at the conjugate point.[50] The resulting dislocation forces are

$$f_1^D = -\frac{Gb_3^2}{2\pi}\frac{a^2}{d(d^2-a^2)},$$

$$f_1^L = -\frac{Gb_3^2}{2\pi}\frac{d}{d^2-a^2}. \qquad (40)$$

The minus sign indicates that they are directed towards the void. The method of image dislocations can also be used to determine the dislocation force on a screw dislocation near a cylindrical circular inhomogeneity.[45,49]

7. DISCUSSION

We included in this paper three different approaches to the derivation of the expression for the energetic force on a straight dislocation: the classical virtual work approach, the potential energy approach which incorporates the effects of image stresses, and the approach based on the evaluation of the J integral. The virtual work approach is the simplest and requires the least amount of mechanics and mathematics background. Its two-dimensional variant presented in section 3 can be readily covered in senior level undergraduate courses of mechanical behavior of materials, advanced mechanics of materials, and mechanics of nanomaterials, which are offered in mechanical engineering, materials science, and nano-engineering curricula. The potential energy approach is more general and conceptually more involved, because it incorporates in the analysis the effects of image stresses. Their contribution to dislocation force must be accounted for whenever a dislocation is close to an inhomogeneity, void, grain boundary, or external boundary of the body. This has been illustrated by several appealing examples which are sufficiently simple to be included in undergraduate coverage of the topic. These include determination of the dislocation force on straight dislocations near slipping and fixed boundaries of an elastic isotropic half-space, or near a cylindrical circular void. The third utilized approach is based on the evaluation of the J integral. It is a powerful approach to determine the dislocation force in many cases without solving the entire boundary-value problem at hand, but it is conceptually most involved and requires the mechanics background that is gained only at the graduate level of engineering or physics education. The presented examples of the determination of glide and climb dislocation forces are sufficiently simple to allow closed-form analytical solutions. For dislocations in material bodies with more complicated boundaries, and for more complex loadings, dislocation force can in general be determined only numerically. For example, to determine dislocation force on an edge or screw dislocation near a surface step of a half-space

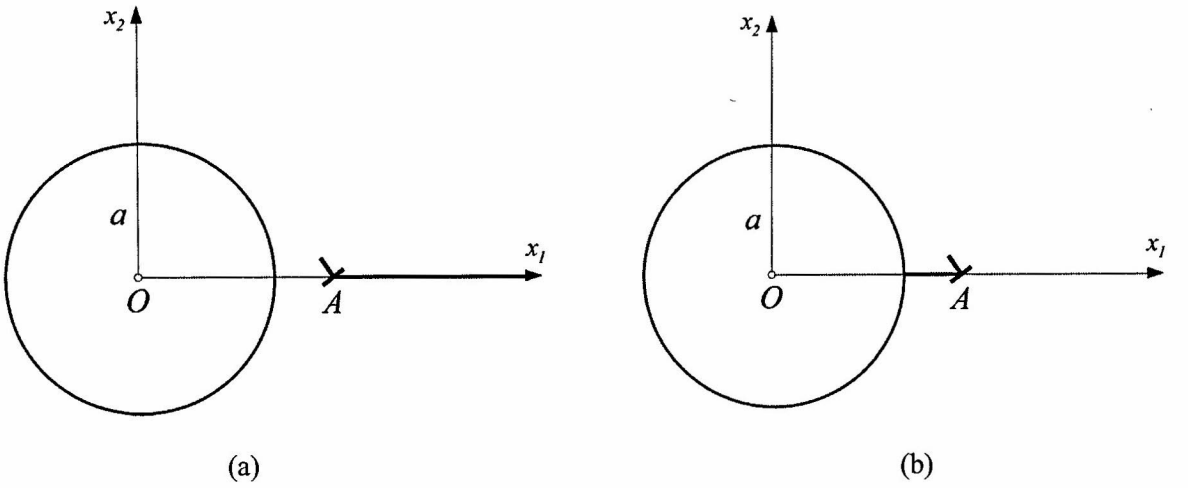

Figure 11. A straight dislocation of a Burgers vector $\{b_1, b_2, b_3\}$ at a distance $OA = d > a$ from the center of a circular void of radius a. In part (a) dislocation is created by displacement discontinuity along the x_1 axis from point A to infinity, while in part (b) displacement discontinuity is imposed from the surface of the void to the dislocation at A.

(Fig. 11a), or near a half-space weakened by a semi-circular groove (Fig. 11b), the finite element method can be used to calculate the stress field due to image tractions used to cancel the infinite-medium tractions over the stepped or grooved boundary of a half-space.[19,49] The so-calculated stresses can then be incorporated into the Peach–Koehler expression for the dislocation force. Such calculations are of importance for the analysis of dislocation nucleation from surface steps,[56,57] or the analysis of inelastic material response which may depend on attractive vs. repulsive effects of surface steps on the dislocation motion.[58,59] Even more complex geometries, involving large number of dislocations, have been considered in the so-called dislocation based plasticity,[60,61] in which plastic deformation is determined as a consequence of collective motion of a large number of discrete dislocations. Kinetic rules are specified for the nucleation and annihilation of dislocations, their motion over obstacles or through grain boundaries, etc. This approach is aimed to explain the formation of organized dislocation structures, such as dislocation walls and cells, and to predict the resulting plastic response of crystalline materials.

ACKNOWLEDGEMENTS

Discussions with Professor Marc A. Meyers from the Materials Science Program of the University of California, San Diego and helpful comments and suggestions by anonymous reviewers are gratefully acknowledged. I also thank Kun Qian, an undergraduate student from the NanoEngineering Department of UC San Diego, for her help in technical preparation of the manuscript.

REFERENCES

1. M.F. Ashby and D.R.H. Jones, *Engineering Materials 1*, 2nd ed., BH, Oxford (2000).
2. D.R. Askeland, P.P. Fulay and W.J. Wright, *The Science and Engineering of Materials*, 6th ed., CL Engineering (2010).
3. W. Brostow and H.E. Hagg Lobland, *Materials: Introduction and Applications*, John Wiley & Sons, New York (2017).
4. W.D. Callister, Jr. and D.G. Rethwisch, *Materials Science and Engineering: An Introduction*, 9th ed., John Wiley (2013).

5. M.A. Meyers and K.K. Chawla, *Mechanical Behavior of Materials*, 2nd ed., Cambridge Univ. Press, Cambridge (2008).
6. A.H. Cottrell, *Dislocations and Plastic Flow in Crystals*, Oxford Univ. Press, London (1961).
7. F.R.N. Nabarro, *Theory of Crystal Dislocations*, Dover Publications, New York (1967).
8. D. Hull and D.J. Bacon, *Introduction to Dislocations*, 5th ed., Elsevier, Amsterdam (2011).
9. P.M. Anderson, J.P. Hirth and J. Lothe, *Theory of Dislocations*, 3rd ed., Cambridge Univ. Press, New York (2017).
10. W. Cai and W.D. Nix, *Imperfections in Crystalline Solids*, Cambridge Univ. Press, Cambridge (2016).
11. R.D. Doherty, *J. Mater. Ed.* **6**, 841 (1984).
12. N.A. Fleck, G.M. Muller, M.F. Ashby and J.W. Hutchinson, *Acta Metall. Mater.* **42**, 475 (1994).
13. V.A. Lubarda, *Mechanics of Materials: Plasticity, Reference Module in Materials Science and Materials Engineering*, Elsevier, 2016, page 24.
14. J.D. Eshelby, *Proc. Roy. Soc. Lond. A* **241**, 376 (1957).
15. R.M. Christensen, *Mechanics of Composite Materials*, John Wiley & Sons, New York (1980).
16. G.Z. Voyiadjis and P.I. Kattan, *Mechanics of Composite Materials with MATLAB*, Springer-Verlag, Berlin (2005).
17. R. Prasad, *J. Mater. Ed.* **25**, 113 (2003).
18. D.K. Roylance, C.H.M. Jenkins and G.E Dieter, *J. Mater. Ed.* **21**, 145 (1999).
19. C.B. Garcia, C.K. Endo, M. Chang and G.E. Beltz, *J. Mater. Ed.* **21**, 149 (1999).
20. M. Peach and J.S. Koehler, *Phys. Rev.* **80** (3), 436 (1950).
21. S.D. Gavazza and D.M. Barnett, *Scripta Metall.* **9**, 1263 (1975).
22. J.D. Eshelby, In *Mechanics of Solids: The Rodney Hill 60th Anniversary Volume*, ed. H.G. Hopkins and M.J. Sewell, Pergamon Press, Oxford, 1982, page 185.
23. V.A. Lubarda, J.A. Blume and A. Needleman, *Acta Metall. Mater.* **41**, 625 (1993).
24. V.A. Lubarda, *J. Elasticity* **32**, 19 (1993).
25. V.A. Lubarda, *Int. J. Solids Struct.* **43**, 3444 (2006).
26. J.R. Rice, *J. Appl. Mech.* **38**, 379 (1968).
27. J.K. Knowles and E. Sternberg, *Arch. Ration. Mech. Anal.* **44**, 187 (1972).
28. B. Budiansky and J.R. Rice, *J. Appl. Mech.* **40**, 201 (1973).
29. L.B. Freund and S. Suresh, *Thin Film Materials: Stress, Defect Formation and Surface Evolution*, Cambridge Univ. Press, Cambridge (2003).
30. M.F. Ashby, *Materials Selection in Mechanical Design*, 4th ed., BH, Elsevier, Amsterdam (2011).
31. R.J. Asaro and V.A. Lubarda, *Mechanics of Solids and Materials*, Cambridge Univ. Press, Cambridge (2006).
32. R.H. Taylor, *J. Mater. Ed.* **36**, 139 (2014).
33. J. Friedel, *Dislocations*, Pergamon Press, Oxford (1964).
34. A. Seeger, *Theorie der Gitterfehlstellen. Handbuch der Physik*, Vol. VII-1, ed. S. Flugge, Springer, Berlin, (1955}, pages 383-665.
35. J. Weertman and J.R. Weertman, *Elementary Dislocation Theory*, Macmillan, New York (1964).
36. R. de Wit, *J. Appl. Physics* **39** (1), 137 (1968).
37. J. Dundurs and A.C. Gangadharan, *J. Mech. Phys. Solids* **17**, 459 (1969).
38. J. Dundurs, In *Mathematical Theory of Dislocations*, ed. T. Mura, ASME, New

York, (1969), page 70.

39. J.D. Eshelby, In: *Prospects of Fracture Mechanics*, ed. G.C. Sih, Noordhoff, Leyden, The Netherlands, 1975, page 69.
40. L.B. Freund, *Int. J. Solids Struct.* **14**, 241 (1978).
41. J.R. Rice, In *Fundamentals of Deformation and Fracture*, eds. B.A. Bilby, K.J. Miller and J.R. Willis, Cambridge University Press, 1985, page 33.
42. A.K. Head, *Proc. Phys. Soc. Lond.* **B66**, 793 (1953).
43. R. Kienzler and H. Kordisch, *Int. J. Fracture* **43**, 213 (1990).
44. V.A. Lubarda, *J. Mech. Mater. Struct.* **10**, 317 (2015).
45. D.M. Barnett and J. Lothe, *J. Phys. F: Metal Phys.* **4**, 1618 (1974).
46. V.A. Lubarda, *Proc. Montenegrin Acad. Sci. Arts* **22**, 1 (2017).
47. V.A. Lubarda, *Int. J. Solids Struct.* **34**, 1053 (1997).
48. R.J. Asaro, *J. Phys. F: Metal Phys.* **5**, 2249 (1975).
49. V.A. Lubarda, *Meccanica*, https://doi.org/10.1007/s11012-017-0693-2 (2017).
50. V.A. Lubarda, J. Elasticity **52**, 289 (1999).
51. V.A. Lubarda and X. Markencoff, *Mater. Sci. Eng. A* **349**, 327 (2003).
52. V.A. Lubarda, *Int. J. Solids Struct.* **48**, 648 (2011).
53. V.A. Lubarda, M.S. Schneider, D.H. Kalantar, B.R. Remington and M.A. Meyers, *Acta Mater.* **52**, 1397 (2004).
54. V.A. Lubarda, *Int. J. Plasticity* **27**, 181 (2011).
55. S.P. Timoshenko and J.N. Goodier, *Theory of Elasticity*, 3rd ed., McGraw-Hill, New York (1970).
56. S. Brochard, P. Beauchamp and J. Grilhé, *Phil. Mag.* **80**, 503 (2000).
57. J. Godet, P. Hirel, S. Brochard and L. Pizzagalli, *Phys. Status Solidi A* **206**, 1885 (2009).
58. F.R.N. Nabarro, In *Surface Effects in Crystal Plasticity*, eds. R.M. Latanision and J.T. Fourie, Noordhoff, The Netherlands, 1977, page 49.
59. D. Kouris, Y. Arai, T. Yamaguchi and E. Tsuchida, *Math. Mech. Solids* **13**, 336 (2008).
60. E. Van der Giessen and A. Needleman, *Modell. Simul. Mater. Sci. Eng.* **3**, 689 (1995).
61. A. Needleman, *Acta Mater.* **48**, 105 (2000).